

## 2017 SNMMI Highlights Lecture: Oncology, Part 2

Wolfgang Weber, MD, Technical University of Munich, Germany

*From the Newsline Editor: The Highlights Lecture, presented at the closing session of each SNMMI Annual Meeting, was originated and presented for more than 30 years by Henry N. Wagner, Jr., MD. Beginning in 2010, the duties of summarizing selected significant presentations at the meeting were divided annually among 4 distinguished nuclear and molecular medicine subject matter experts. Each year Newsline publishes these lectures and selected images. The 2017 Highlights Lectures were delivered on June 14 at the SNMMI Annual Meeting in Denver, CO. In this issue we feature the second part of the lecture by Wolfgang Weber, MD, professor and chair of Nuclear Medicine at the Technical University of Munich (Germany), who spoke on highlights in oncology. The first part appeared in the January 2018 (most recent) issue of Newsline. Note that in the following presentation summary, numerals in brackets represent abstract numbers as published in The Journal of Nuclear Medicine (2017;58[suppl 1]).*

**B**ecause of the success of  $^{177}\text{Lu}$ -prostate-specific membrane antigen (PSMA)-617 in the treatment of prostate cancer, we are now seeing a great deal of interest in making even better therapeutic agents targeting PSMA-positive cancer cells. One interesting approach is not to further improve affinity for PSMA but, instead, to modify the clearance rate from the blood. Ling et al. from the University of Pittsburgh (PA) and Cancer Targeted Technology (Woodinville, WA) reported on “Comparison of traditional and albumin-binding  $^{177}\text{Lu}$ -labeled phosphoramidate-based PSMA inhibitors for targeted radionuclide therapy of prostate cancer” [317]. These researchers have introduced this albumin-binding motif in a PSMA ligand and shown in preclinical studies that, as expected, it significantly increased the time that this agent remained in the circulation in a mouse model. However, it also increased tumor uptake, which continued to increase up to 48–72 hours after injection (up to 50% ID/g in the tumor) and increased therapeutic efficacy. Five of 8 animals receiving the albumin-binding agent survived for >200 days past tumor implant, probably as a result of significantly higher tumor uptake; only 2 mice experienced a regrowth of disease. Of course, one concern is the fact that radiation exposure to the bone marrow increases with this longer circulation time. At least in this mouse model this does not seem to have been a major problem. Survival was significantly better among animals that received the PSMA ligand that stayed longer in the circulation.

We can also modify PSMA agents for therapy by using different radioisotopes, and much interest is currently focused on the use of  $\alpha$  emitters for treatment of prostate cancer and on comparison of outcomes with those from  $\beta$

emitters, which have been studied more extensively. Ray et al. from the Johns Hopkins Medical Institution/University (Baltimore, MD) reported on “Low- and high-linear energy transfer (LET) radiometal-based therapeutics for prostate cancer” [312]. Among other radionuclides, they compared the efficacy of  $^{225}\text{Ac}$ - and  $^{177}\text{Lu}$ -labeled PSMA ligands in a preclinical model of metastatic castration-resistant prostate cancer. Survival was enhanced and the rate of tumor growth significantly better controlled with the  $\alpha$ -emitting (actinium-labeled) compound than with the  $\beta$ -emitting (lutetium-labeled) compound. This suggests that actinium and possibly other  $\alpha$  emitters have significant potential for treatment of prostate cancer. In this study, the authors also concluded that PSMA-targeted low- and high-LET radiopharmaceutical therapies enable improved survival in mice bearing primary tumor xenografts, whereas high-LET radiopharmaceutical therapy is promising in treating micrometastases after systemic administration.

Again, other targets are being studied, and here I am returning to the gastrin-releasing peptide receptor (GRPR), the alternative target in prostate cancer. Okoye et al. from the University of Iowa (Iowa City), the University of Missouri (Columbia), and the U.S. Department of Veterans Affairs (Columbia, MO) reported on “Targeting the BB2 receptor in prostate cancer using a  $^{203}\text{Pb}$ -labeled peptide” [321]. They evaluated the compound  $^{203}\text{Pb}$ -RM2, a BB2 receptor antagonist, for targeting BB2 receptor-expressing prostate cancer in PC-3-xenografted animal models.  $^{203}\text{Pb}$  is, of course, used for imaging purposes and is combined with the GRPR-binding ligand RM2 (Fig. 1). Although perhaps difficult to see in the  $^{203}\text{Pb}$ -RM2 images (left) in a tumor-bearing mouse, only a minute amount of kidney uptake is visualized at 24 hours postinjection (left), so that everything else on the images is tumor uptake. In the images in which the lead agent was not attached to RM2 (right), bowel distribution is visualized along with uptake in the kidneys and bones.  $^{203}\text{Pb}$  compounds may prove to be suitable imaging companions for  $^{212}\text{Pb}$  therapy agents, including both GRPR and PSMA ligands.

Much interest is also focused on developing antibodies for treatment of various diseases. Many antibodies are entering the clinic in their unlabeled form, and many are excellent vehicles for radioisotope therapy. One challenge is their long circulation in the blood, which results in high bone marrow doses, but this can be overcome by pretargeting strategies. Cheal et al. from the Memorial Sloan Kettering



Wolfgang Weber, MD

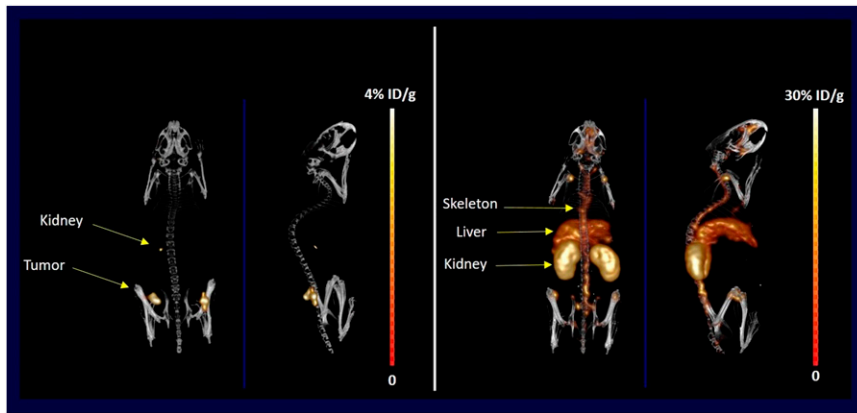


**FIGURE 1.** Targeting the BB2 receptor in prostate cancer using a  $^{203}\text{Pb}$ -labeled peptide.  $^{203}\text{Pb}$ -RM2, a BB2 receptor antagonist, was used to target BB2 receptor-expressing prostate cancer in PC-3-xenografted murine models and in normal mice. Left:  $^{203}\text{Pb}$ -RM2 in tumor-bearing SCID mouse. Only a minute amount of kidney uptake was visualized at 24 hours postinjection, so that all other uptake in this image is in tumor. Right:  $^{203}\text{PbCl}_2$  in a CF-1 normal mouse. Bowel distribution was visualized at 24 hours, along with uptake in the kidneys and bones.

Cancer Center (New York, NY) and the Massachusetts Institute of Technology (Cambridge, MA) reported on “Comparative efficacy and toxicity of  $^{177}\text{Lu}$ - vs  $^{90}\text{Y}$ -theranostic anti-HER2/anti-DOTA(metal) pretargeted radioimmunotherapy (anti-HER2 DOTA-PRIT) of HER2-expressing breast cancer xenografts with curative intent” [54]. They used a radionuclide pretargeting strategy with antichelate antibodies, showing that 3-step pretargeting of radioactive hapten to HER2-positive xenografts was possible using a new class of bispecific antibody (IgG-scFv). This antibody binds to HER2 with 2 arms and another arm binds to DOTA. Therapy is performed by first injecting the antibody, giving it some time to clear, and then injecting only the DOTA (labeled with  $^{90}\text{Y}$  or  $^{177}\text{Lu}$ ). In this study, the  $^{177}\text{Lu}$ -DOTA-Bn bound to the antibody was quite effective in human breast cancer BT-474-xenografted mice. The investigators showed significant tumor shrinkage and even cure (75%) with both  $^{90}\text{Y}$ - or  $^{177}\text{Lu}$ -antibodies, but the lutetium antibody was better tolerated with superior outcomes in this mouse model.

Thus far in this lecture we have looked only at agents that target specifically. We should also remember that in some instances it may be helpful to locally administer radioisotopes. This is especially true in the brain, where tumors always recur locally, so that local injection of radioisotopes is a logical and interesting strategy. Bao et al. from the Seidman Cancer Center at Case Western Reserve University (Cleveland, OH) and colleagues at the University of Texas Health Science Center (San Antonio) and Alamo Isotopes (Somerset, TX) reported on “First-in-human study of  $^{186}\text{Re}$ -nanoliposomes ( $^{186}\text{RNL}$ ) delivered intratumorally by convection-enhanced delivery for treatment of recurrent glioblastoma: Safety, image biodistribution, and radiation dosimetry” [599]. These researchers used nanoparticles encapsulating  $^{186}\text{Re}$  in 3 dose cohorts (1, 2, and 4 mCi), injected this locally under image guidance, and studied biodistribution with serial whole-body planar gamma camera and SPECT/CT brain imaging acquired for 8 days after administration of the agent. Baseline and follow-up MR images were also acquired and coregistered to the SPECT/CT data. They saw a decrease in contrast enhancement on follow-up images, which nicely corresponded to the distribution of

the radiolabeled nanoliposomes and indicated treatment response (Fig. 2). The procedure was safe, and no significant toxicity was noted at these doses.

We have talked about molecules, targeting, radioactivity, and treatment aspects. To expand our view of therapeutic applications in nuclear medicine a little bit farther, I wanted to also include this interesting abstract from Yoshii et al. from the National Institute of Radiological Sciences and the National Institutes for Quantum and Radiological Science and Technology (Chiba, Japan), the National Cancer Center (Tokyo, Japan), and Nihon Med-Physics Co., Ltd. (Tokyo, Japan), who reported on “Feasibility of a PET-guided surgery system with  $^{64}\text{Cu}$ -PCTA-cetuximab for accurate resection of intraperitoneal tumors in a mouse model of peritoneal dissemination” [528]. They have developed a real-time PET imaging system for surgical guidance. Human colon cancer HCT116 cells stably expressing red fluorescent protein were intraperitoneally seeded into mice. At 1 week after cell inoculation,  $^{64}\text{Cu}$ -PCTA-cetuximab was administered intraperitoneally. PET-guided surgery

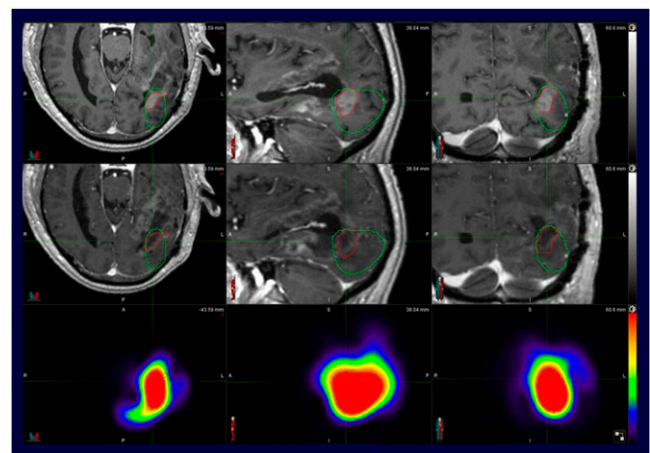


**FIGURE 2.** Intratumorally administered  $^{186}\text{Re}$ -nanoliposomes in recurrent glioblastoma. Patient received 4 mCi administered under image guidance. Top row: baseline MR images; middle row, MR images at 1 month showing treatment response covering the area of  $^{186}\text{Re}$ -nanoliposome distribution; bottom row: SPECT imaging showing tumor uptake at 24 hours.

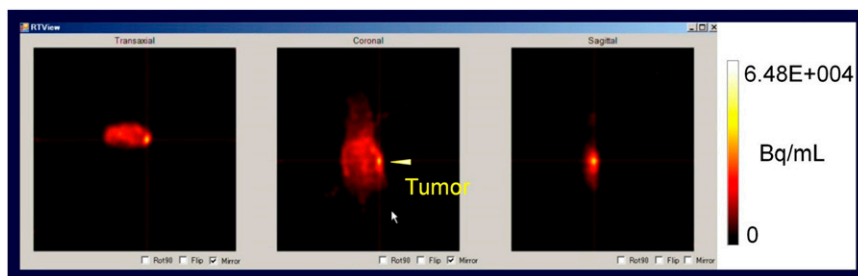


**FIGURE 3.** OpenPET-guided surgery with  $^{64}\text{Cu}$ -PCTA-cetuximab in a mouse model. Left to right: transaxial, coronal, and sagittal images of a small 3-mm tumor identified by PET in the peritoneal cavity.

was performed 24 hours later. High-speed reconstruction enabled updating of images in  $<1$  second, allowing the surgeons to see precisely where they were cutting in relation to accumulation of tracer in the mouse. Figure 3 is an example in a mouse in which a 3-mm tumor was visualized and then resected using this device.

### Imaging Cancer Immunotherapy

Imaging of cancer immunotherapy was a major focus at this year's SNMMI meeting. Cancer immunotherapy was considered to be a breakthrough in medicine only a few years ago, and it remains a major topic of interest, with many antibodies entering the field. However, applications of these antibodies all struggle with one problem that has been well described in the literature. Although about 20%–30% of patients will benefit enormously from these treatments with longtime regression of their disease, most patients are not responders. So in many studies, we see that 20%–30% may be in a longer-surviving group, whereas other patients die quickly. The question is: can we use imaging to better study this and identify why these treatments are or are not working? This remains an unsolved problem and challenge to researchers who want to advance these therapies. We now have several tools for cancer immunotherapy, with several

U.S. Food and Drug Administration (FDA)–approved antibodies. Two approved antibodies, nivolumab and pembrolizumab, target programmed cell death receptor 1 (PD-1), which is predominantly expressed on lymphocytes in the tumor tissue. We also have 2 antibodies, atezolizumab and avelumab, approved for the PD-1 ligand PD-L1, which is predominantly expressed on cancer cells. In addition, ipilimumab targets cytotoxic T-lymphocyte–associated protein 4 (CTLA-4), which is expressed mostly on inhibitory T-cells. Again the questions are: can we use these antibodies to study the expression of these important target molecules, and can this imaging potentially predict whether or not immunotherapy will be effective?

It was very encouraging at this meeting to see that so much research is ongoing in this area and that promising data are being accrued on the many different aspects of all these targets for immunotherapy. Jiang et al. from the University of Wisconsin–Madison reported on “Targeted programmed cell death-1 receptor (PD-1) expression in lung cancer using a humanized mouse model” [179]. These researchers described the development of  $^{89}\text{Zr}$ -Df-nivolumab for mapping the biodistribution of activated PD-1–expressing T-cells in a murine model of lung cancer. After establishment of tumors and later injection of human lymphocytes, mice were injected with the

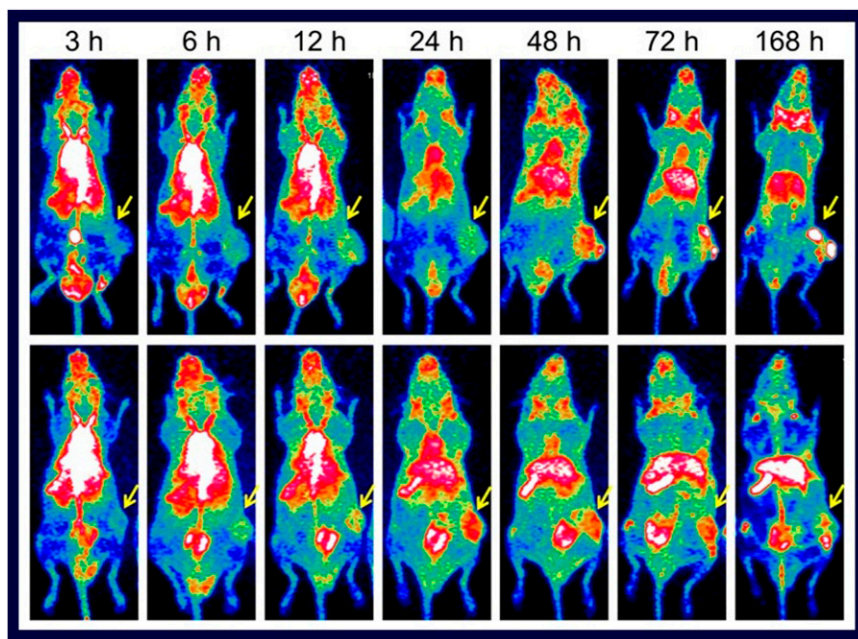


**FIGURE 4.** PET imaging of PD-1 in a murine model of lung cancer at (left to right) 3, 6, 12, 24, 46, 72, and 168 hours after injection of  $^{89}\text{Zr}$ -Df-nivolumab to map biodistribution of activated PD-1–expressing T-cells. Top row: humanized mouse model; bottom row: nonhumanized mice.

tracer and underwent serial PET imaging for up to 168 hours after injection (Fig. 4). The biodistribution of the tracer reflected PD-1 expression, as confirmed by subsequent fluorescence immunohistochemistry. What the study also showed was that specific uptake in these lymphocytes occurred only relatively late (several days after injection), whereas at earlier time points antibody uptake was similar to that of an antibody in which no specific binding occurred or to uptake in a model with no human lymphocytes injected. The authors concluded that “this tracer holds great promise to aid in further understanding of immune checkpoint blockade therapy and the development of future PD-1–targeted imaging strategies and may come to be a useful tool in the understanding and further exploration of immune checkpoint inhibition treatments.”

We also saw several presentations on imaging of PD-L1 at this meeting. Jagoda et al. from the National Cancer Institute and the National Institutes of Health (Bethesda and Rockville, MD) and Leidos Biomedical Research Inc. (Frederick, MD) reported on “Immuno-PET imaging of PD-L1 using the therapeutic monoclonal antibody, avelumab” [178]. In a tumor model of PD-L1–positive tumors, they studied the impact of the antibody mass on the signal. It is quite important to understand that for antibody imaging, the mass of antibody injected has a major impact on the image that can be generated, which is different from the

small molecules on which we currently focus in nuclear medicine. In this study, the researchers labeled avelumab with  $^{89}\text{Zr}$  and evaluated it in human PD-L1–expressing cancer cells and mouse xenografts to understand appropriate PD-L1 targeting and the potential for clinical translation. They showed dramatic effects on uptake in normal organs, such as the spleen, with uptake drastically reduced with increasing antibody mass. However, at the same time, uptake in the tumor was increasing, probably because the sink of antibody in the spleen was decreased. Even more complex was uptake in the lymph nodes, with a peak and then decreasing. These authors concluded that clinical PET imaging with this agent may have value in identifying patients who may benefit from PD-L1 immunotherapies. The data also indicated that uptake of this agent in PD-L1 tumors may be increased with appropriate PD-L1 monoclonal antibody protein loading, which would improve detection of PD-L1–positive lesions in humans.

Another presentation with a similar focus came from Ehlerding et al. from the University of Wisconsin–Madison, who reported on “ImmunopET of CTLA-4 expression in murine models of non–small cell lung cancer (NSCLC)” [181]. The researchers described the use of a zirconium-labeled antibody,  $^{89}\text{Zr}$ -Df-ipilimumab, in *in vitro*, *in vivo*, and *ex vivo* studies in 3 NSCLC lines (A549, H460, and H358). They showed uptake in tumors (Fig. 5), representing expression of CTLA-4 on tumor cells, which is currently not well understood. PET imaging may also be able to detect this in patients, a fact of special interest because ipilimumab is an FDA-approved antibody.

The disadvantage of these antibodies, despite the fact that they have high specificity for target binding and are already FDA approved as therapeutics so that the hurdles of entering the clinic are relatively low, is that imaging must be performed several days after injection. Can we design smaller molecules that allow us to perform same-day imaging and thereby use radioisotopes, like  $^{18}\text{F}$ , that are more readily available? Donnelly et al. from Bristol–Myers Squibb (Princeton, NJ, and Waltham, MA) reported on “Discovery of a novel  $^{18}\text{F}$  prosthetic group that enables radiolabeling of anti-human PD-L1 adnectins” [68]. Small molecules bind with picomolar affinity to human PD-L1, and these researchers showed that the small protein they developed,  $^{18}\text{F}$ -BMS-986192, was bound with high affinity in human non–small cell lung cancer tissue samples. In addition to describing the development and *in vitro* studies with this  $^{18}\text{F}$ -labeled anti-PD-L1 adnectin, the group also performed same-day studies in mice (Fig. 6). They demonstrated high uptake in PD-L1–expressing tumors and showed that uptake was completely blocked by injection of the cold compound, indicating that this is a promising compound for studying PD-L1 expression in patients, with the significant advantage that PET imaging can be performed on the same day as tracer injection.

So far we have looked only at examples of more or less static imaging of immune response—the expression of

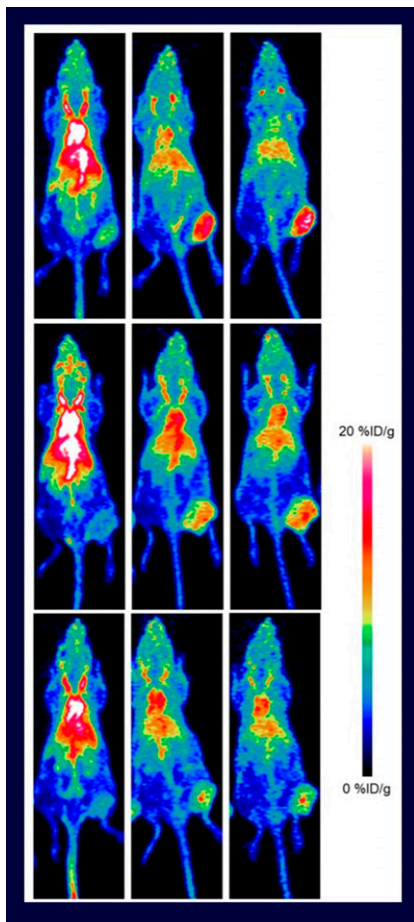


**FIGURE 5.** ImmunopET of CTLA-4 expression on human non–small cell lung cancer (NSCLC) cells transplanted into mice. Mice shown bearing NSCLC lines (top to bottom) A549, H460, and H358 at (left to right) 3, 24, and 48 hours after radiolabeled antibody injection. The intensity of tracer uptake on PET correlated with the expression level of CTLA-4 as determined by Western blotting.

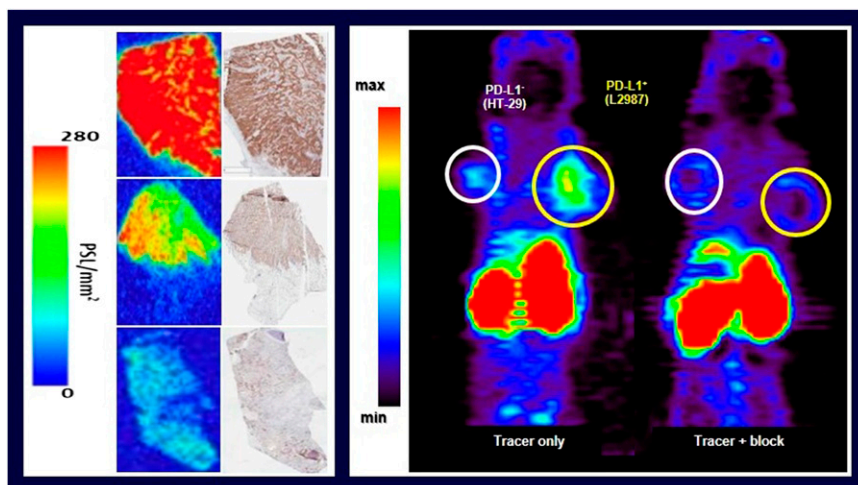


**FIGURE 6.**  $^{18}\text{F}$ -labeled PET imaging of PD-L1-expressing non-small cell lung cancer (NSCLC) tumors in mice with (left)  $^{18}\text{F}$ -BMS-986192 only and (right) with the tracer plus a blocking dose. This approach carries the significant advantage of enabling same-day imaging of PD-L1 expression in patients.

these targets. If we are targeting this expression as part of a strategy to activate the immune system, then we also want to be able to see the action of the activated lymphocytes. One interesting way to do this is to look at an enzyme called granzyme B, which is released by activated lymphocytes and is critical in induction of apoptosis in cancer cells. Larimer et al. from the Massachusetts General Hospital (Boston and Charlestown, MA) reported that “A novel granzyme B PET-imaging peptide is predictive of immunotherapy response” [182]. Mice bearing the syngeneic CT26 murine colon cancer cell line were used for biomarker analysis and murine imaging. Mice were treated with either an anti-PD-1 agent or in combination with anti-CTLA-4 therapy on days 3, 6, and 9 after inoculation. Tumors were measured every 2–3 days, and PET images were acquired at day 12. They performed ex vivo analyses of treated and untreated tumor-bearing mice and showed significant differences in granzyme B in treated and untreated mice (Fig. 7).

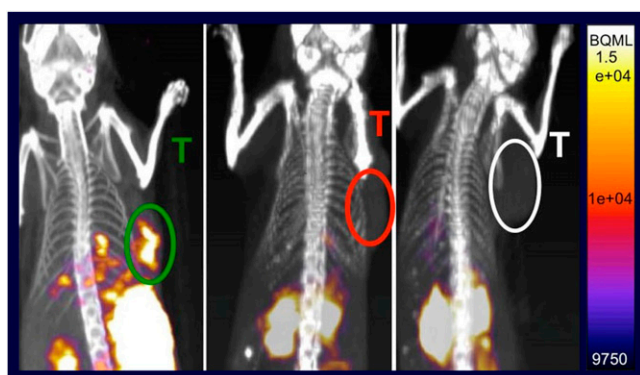


**FIGURE 7.** Granzyme B PET imaging and immune response prediction. Imaging in mice bearing syngeneic CT26 murine colon cancer cell line tumors and (left) treated with and responding to the novel granzyme B PET imaging peptide; (middle) treated but nonresponding; and (right) treated with vehicle only. These results and preliminary results in human samples indicate that granzyme B imaging is a promising predictive PET biomarker for use with immunotherapies.

They also showed that when the treatment was effective then tumor uptake was higher than background, whereas when there was no response then uptake was not increased. Nor was uptake above background seen when treatment was with vehicle alone, because the lymphocytes in the tumor were not activated. Although the overall signal is relatively small, these studies indicate the feasibility of using granzyme B to detect not only the presence of target and lymphocytes but also their activation status.

With all of these imaging probes, again, it is important to perform careful systematic evaluations. One reason was illustrated by the presentation from Ikotun et al. from Amgen, Inc. (Thousand Oaks and South San Francisco, CA), who reported on “A targeted PET probe approach for noninvasive imaging of cytotoxic lymphocytes” [184]. These researchers developed a CD8 antibody fragment tracer with the intention of detecting and monitoring tumor-infiltrating lymphocytes in response to immunotherapy. They used the anti-mouse CD8 F(ab')<sub>2</sub> PET probe before and after 4-1BB-directed immunotherapy. They observed that this immune-stimulating treatment resulted in an increased uptake of the CD8-specific antibody fragment in tumor-draining lymph nodes, consistent with immune activation. However, tumor uptake of the antibody fragment was not significantly increased by 4-1BB-directed immunotherapy. Furthermore, CD8 depletion did not decrease the uptake of the CD8-specific antibody fragment in the tumor tissue, and a nonspecific control antibody showed similar tumor uptake (Fig. 8). So uptake in the tumor tissue was not reflecting specific binding to CD8 for this antibody fragment. This is a reminder that, although these are very interesting tracers, we must also be careful to evaluate them critically and not consider every focal accumulation as proof that we are visualizing our targets.

### Many Other Interesting Abstracts

To conclude, I would like to look at a few of the other interesting presentations outside of prostate cancer and immunotherapy at this meeting that did not fit in the previous categories.

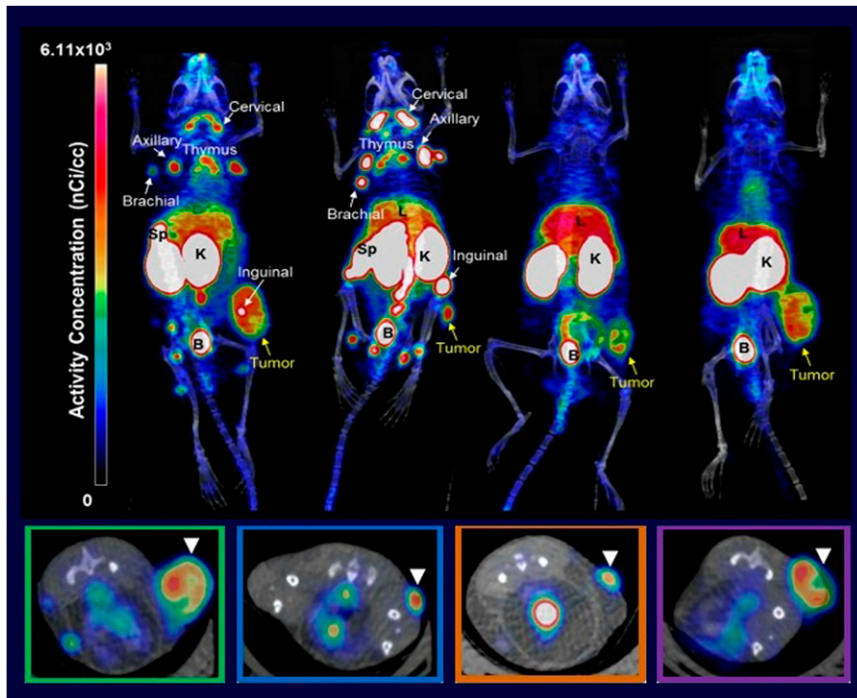


**FIGURE 8.** Targeted PET probe approach for noninvasive imaging of CD8-positive lymphocytes. 4-1BB therapy increased the activity concentration in lymph nodes but not in tumor tissue. Uptake of CD8 $\alpha$  in the tumor tissue appears nonspecific, because it is similar to the control antibody fragment and not decreased by CD8 depletion.

One was again based on antibody imaging, but focused on antibody target CA 19-9, which is overexpressed in various tumors. Lohrmann et al. from the Memorial Sloan Kettering Cancer Center (New York, NY) and MabVax Therapeutic Holdings, Inc. (San Diego, CA) reported on a “First-in-human study of  $^{89}\text{Zr}$ -DFO-HuMab-5B1 (MVT-2163) PET/CT imaging with and without HuMab-5B1 (MVT-5873) in patients with pancreatic cancer and other

CA 19-9–positive malignancies” [385]. We studied this in a phase I trial in a group of patients with metastatic pancreatic cancer and were able to clearly visualize lymph node metastases. The results of this study again illustrate the importance of taking into account the antibody mass. At the lower injected mass, very intense uptake was seen in liver and spleen, which limits detection of liver metastases. However, by coinjection of the cold antibody we were able to visualize liver metastases also at high contrast (Fig. 9).

Small molecules were also presented at this meeting with very interesting potential applications, including imaging of PARP-1, which is a DNA repair enzyme. PARP inhibitors have been recently approved for treatment of metastatic ovarian cancer. The question is: can we use these

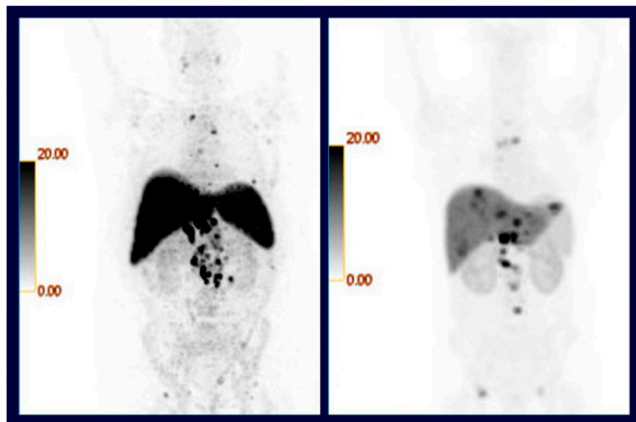


**FIGURE 9.** Maximum-intensity projection  $^{89}\text{Zr}$ -DFO-HuMab-5B1 (MVT-2163) images in patients with metastatic pancreatic cancer demonstrating the effects of an HuMab-5B1 (MVT-5873) cold antibody predose. Left: With 3 mg  $^{89}\text{Zr}$ -DFO-HuMab-5B1; right, with 47 mg MVT-5873 and 3 mg  $^{89}\text{Zr}$ -DFO-HuMab-5B1. The lower injected mass of the tracer alone resulted in very intense uptakes in liver and spleen, which limited detection of liver metastases. Coinjection of the cold antibody decreased liver and spleen uptake of the antibody and allowed for visualization of liver metastases. Images are from different patients.

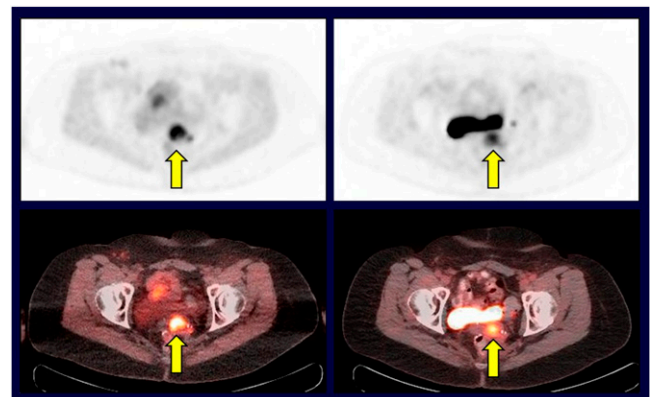


**FIGURE 10.** Comparison images acquired with a novel PET tracer,  $^{18}\text{F}$ -FTT (left), and  $^{18}\text{F}$ -FDG (right) in a patient with metastatic ovarian carcinoma.  $\text{SUV}_{\text{max}}$  on  $^{18}\text{F}$ -FTT correlated with PARP-1 immunohistochemistry.

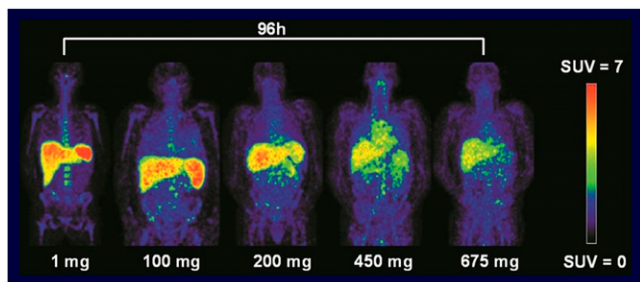


**FIGURE 11.** Dose-dependent uptake of  $^{89}\text{Zr}$ -anti-CD44 (RG7356) by normal organs in patients with advanced CD44-expressing solid tumors at doses (left to right) of 1, 100, 200, 450, and 675 mg. Depending on the injected mass, normal tissue uptake of  $^{89}\text{Zr}$ -anti-CD44 (RG7356) varied widely. PET can be used to noninvasively assess the impact of antibody mass on tissue distribution.

as a basis for imaging agents for PARP expression, and do the degree of PARP expression and uptake of the imaging probe correlate with response to treatment? Pantel et al. from the University of Pennsylvania (Philadelphia) demonstrated that this was feasible in their report on “A pilot study of a novel poly (ADP-ribose) polymerase-1 (PARP) PET tracer ( $^{18}\text{F}$ -FluorThanatrace;  $^{18}\text{F}$ -FTT) in patients with ovarian carcinoma” [386]. The study included 17 such patients, and imaging results with  $^{18}\text{F}$ -FTT were compared with those from  $^{18}\text{F}$ -FDG. Figure 10 shows comparison imaging with  $^{18}\text{F}$ -FTT (left) and  $^{18}\text{F}$ -FDG (right) in a patient with metastatic ovarian cancer, with focal uptake enhanced on  $^{18}\text{F}$ -FTT PET.  $\text{SUV}_{\text{max}}$  on  $^{18}\text{F}$ -FTT correlated with PARP-1 immunohistochemistry in tissue samples, whereas no correlation was seen with  $\text{SUV}_{\text{max}}$  on  $^{18}\text{F}$ -FDG. The authors concluded that these preliminary results suggest that  $^{18}\text{F}$ -FTT holds promise as a noninvasive measure of PARP-1 expression and warrants further study as a predictive biomarker for response to DNA-damaging agents.

Antibodies and PET imaging can be used not only for diagnostic purposes but also to study the distribution of therapeutically administered antibodies. Although this is not yet a clinical application, it represents a promising research application for nuclear medicine, where PET imaging determines whether an unlabeled antibody that is supposed to be used for therapeutic purposes is actually accumulating in tumor tissue and to characterize that accumulation in comparison to normal tissue. Jauw et al. from the VU University Medical Center (Amsterdam, The Netherlands) and Hoffmann La Roche (Basel, Switzerland) reported on “In vivo assessment of antibody selectivity: Immuno-PET with anti-CD44 antibody in a phase I clinical study” [389]. The study included patients with advanced CD44-expressing solid tumors. The researchers showed that, depending on the injected mass, normal tissue uptake of  $^{89}\text{Zr}$ -anti-CD44 (RG7356) (and also potential complications) can vary widely (Fig. 11).

Existing tracers have also found new applications. One example comes from a report at this meeting on a peptide binding to the chemokine receptor CXCR4, which has been used as a target for inflammation imaging and also accumulates in several tumor types. Leisser et al. from the Medical University of Vienna (Austria), the CBmed Zentrum für Biomarkerforschung in der Medizin (Graz, Austria), the Ludwig Boltzmann Gesellschaft (Vienna, Austria), Scintomics GmbH (Fürstenfeldbruck, Germany), and the Technische Universität München (Garching, Germany) reported on “Noninvasive evaluation of CXCR4 expression of mucous-associated lymphoid tissue (MALT) lymphoma using  $^{68}\text{Ga}$ -pentixafor PET/MRI—A prospective study” [563]. MALT lymphomas are often only mildly positive on  $^{18}\text{F}$ -FDG PET imaging, whereas the CXCR4 agent showed very high uptake and high image contrast. Figure 12 is an example image with high uptake in the primary tumor and involved lymph nodes that would be unusual to visualize at this intensity with  $^{18}\text{F}$ -FDG PET.

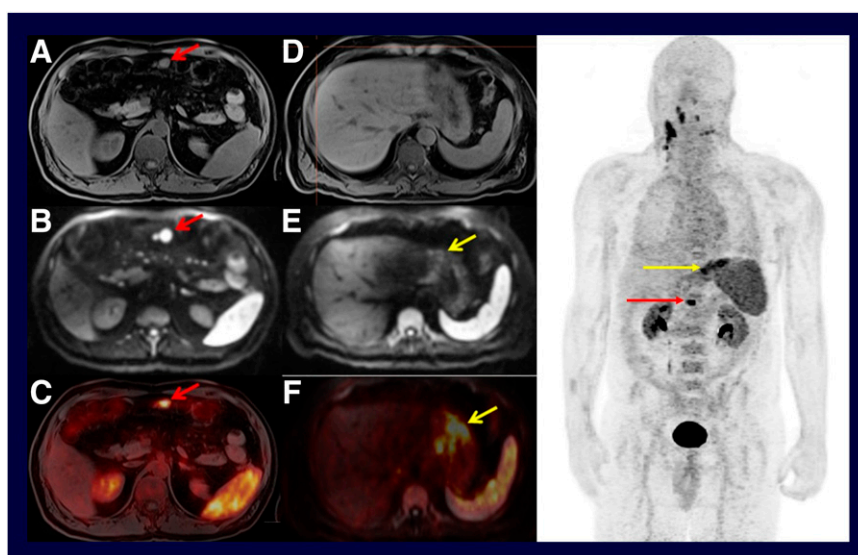


**FIGURE 12.** Detection of MALT lymphoma using the CXCR4 ligand  $^{68}\text{Ga}$ -pentixafor and PET/MR imaging. Left: Images showing a MALT lymphoma in the stomach (yellow arrows) as well as a secondary lesion (red arrows). (A, D): T1-weighted sequence; (B,E): apparent diffusion coefficient mapping; and (C,F) PET/MR fusion images. Right: Whole-body PET MIP.

(Continued on page 17N)

NRP if completed at an institution with a DR program accredited by the ACGME. However, more therapies are required in the modified pathway: “10 oral  $^{131}\text{I}$  NaI  $\leq$  33 mCi, 5 oral  $^{131}\text{I}$  NaI  $>$  33 mCi, and 5 parenteral  $\alpha$  emitter,  $\beta$  emitter, photon emitter  $<$  150 keV.” The requirements and registration for the NRP are available online (5,6). Although a graduate of the NRP is eligible for subspecialty certification in nuclear radiology by the ABR, that DR is not necessarily eligible for certification by the American Board of Nuclear Medicine.

Notwithstanding the recent modifications to the ABR NRP, if the survey is representative of the current state of national adoption, it suggests that the number of programs and the number of residents taking advantage of it are few. The DR respondent programs offering the NRP are medium to large in size, and half have  $\geq$ 41 DR residents. The number of extra lectures, cases, and laboratory time for residents in the NRP is quite varied in comparison to traditional DR programs. In addition, a several-fold variation

is noted in the number of faculty certified in nuclear medicine and/or nuclear radiology at these programs.

## REFERENCES

1. Mankoff DA, Pryma DA. Nuclear medicine training: What now? *J Nucl Med.* 2017;58:1536–1538.
2. Czernin J. Is 16 months of specialized nuclear medicine training enough for best patient care? *J Nucl Med.* 2017;58:1535.
3. Segall GM, Grady EE, Fair JR, Ghesani MV, Gordon L. Nuclear medicine training in the United States. *J Nucl Med.* 2017;58:1733–1734.
4. Oates ME, Guiberteau MJ. Adoption of the 16-month American Board of Radiology pathway to dual board certifications in nuclear radiology and/or nuclear medicine for diagnostic radiology residents. *Acad Radiol.* 2014;21:1348–1356.
5. American Board of Radiology. Diagnostic Radiology Subspecialties. 16-month pathway to dual certification in diagnostic radiology and nuclear radiology. Available at: <https://www.theabr.org/diagnostic-radiology/subspecialties/nuclear-radiology/requirements-registration>. Accessed on November 27, 2017.
6. American Board of Radiology. 16-month pathway to dual certification in diagnostic radiology and subspecialty certification in nuclear radiology. Candidate application. <https://form.jotformpro.com/70243494028959>. Accessed on November 27, 2017.

---

(Continued from page 15N)

I would like to conclude with  $^{18}\text{F}$ -FDG PET and its important applications in lymphoma, where much interesting work remains. It is important, however, that these studies be performed in large, multicenter trials so that we can arrive at definitive answers and consensus on the utility of PET imaging. One example presented at this meeting came from Kobe et al. from the University Hospital of Cologne (Germany), who reported on “Staging Hodgkin lymphoma using PET: Can we safely exclude bone marrow involvement?” [565]. The authors answered this question decisively: in a group of more than 800 patients with Hodgkin lymphoma they found that  $^{18}\text{F}$ -FDG PET correctly identified almost all patients who were positive on bone marrow biopsy and, more important, identified 110 patients who were negative on bone marrow biopsy but had clear bone marrow involvement on PET. This strong evidence suggests that bone marrow biopsy is probably no longer necessary in these patients with Hodgkin lymphoma, and it can be replaced by  $^{18}\text{F}$ -FDG PET imaging.

## Conclusions

Several key observations can be made to summarize some of the results from the more than 400 abstracts presented on oncology at this meeting. One obvious observation is that although FDG was celebrated as the “molecule of the century” in 2016, PSMA (or, as it might be more accurately called, glutamate carboxypeptidase II) is definitely the target of the decade. We should not call it the molecule of the decade, because it is actually an imaging and therapeutic target. Another trend noted at the meeting is the marked increase in interest in radionuclide therapy, especially in the treatment of metastatic prostate cancer. Immuno-PET is also being further developed and studied extensively preclinically, with encouraging results. Several clinical studies in this area are already ongoing. Finally, I believe that the current interest and emphasis on theranostics will expand the field of nuclear medicine and eventually enhance its overall impact on patient care.